Fluid Flow Properties of Slotted Flat- and Hollow-blade Impellers

D. Georgiev and S. D. Vlaev*
Institute of Chemical Engineering, Bulgarian Academy of Sciences,
Acad. G. Bonchev Str., Bl. 103, 1113 Sofia, Bulgaria

Original scientific paper
Received: June 27, 2007
Accepted: January 29, 2008

Published data on flow field variation caused by various blade design patterns are scarce. Most designs exhibit significant flow separation and adverse pressure gradients effects that lower mixing efficiency. In view of the design potentials of the CFD methodology, the flow field variations caused by different blade designs could be classified in order to be able to predict the spread of the low pressure regions behind blades while retrofitting existing equipment towards energy-saving performance without decreasing the impeller blending and dispersing capacity related to the geometry considered. The aim of the present study is to reveal such variations for some conventional flat blade modifications. The performance of three flat and hollow blade design modifications comprising slotted and perforated blades are examined. The specific power drawn, pumping capacity, deformation rate and turbulence intensity are determined and compared. The impeller power effectiveness is discussed in terms of the strain deformation rate produced. Evidence for enhanced performance of slotted and perforated designs is presented.

Key words:
Mixing, modified flat/hollow blades, CFD, impeller characteristics

Introduction

Impeller blade geometry is a basic precondition for effective mixing, as well as an important optimization target. In view of the recent trends towards greenhouse gas limitation,[1] the successful design of a stirrer has become extremely important bearing the insight of possible energy-saving. On the other hand regarding productivity, the spread of composite materials have allowed the realisation of more complex forms and have lifted up the limits on shape. Thus, development of impeller design has remained a priority objective.

While it is impossible to quote all relevant works considering impeller designs, one could refer to a recent interest on blade shape, as manifested in several representative studies.[2–8] Yet, a systematic description of the relationship between shape modification and mixing impeller flow field is lacking. More comparative information is needed in order to be able to discriminate between the properties assigned to different geometry. In view of the design potentials of the computational fluid dynamic (CFD) methodology,[9,10] the flow field variations caused by different blade designs can be classified. In order to allow such classification, the characteristic deviations of impeller flow field parameters caused by typical modifications of the classified blades, e.g. flat, inclined, fluid-foil ones, should be examined. The present study is focused on modified flat and hollow blade designs. Work on blade modifications in a similar context has been reported by Smith and coworkers.[11,12] We have extended these studies by looking at the effect that slots on the blades could produce on the pressure distribution at the blade rear.[13] Design hints of slots were borrowed from the fluid dynamics of airfoils.[14]

The aim of this paper is to characterise the hydrodynamic properties of impellers with slots following a systematic CFD evaluation of the parameters of the blades' flow field.

Experimental

The following procedures were carried out: (1) A RANS model was formulated. (2) The individual impeller cases were solved by the MRF solution procedure. (3) The velocity and the pressure fields around the impellers were revealed; the low pressure regions of the vortex systems were outlined and their relevant power and flow numbers were determined. (4) The power effectiveness of the design modifications related to flow deformation and gas-liquid mass transfer, was compared.

Simulated cases

The analysis was focused on modified flat blades with a background of information regarding their performance in some two-phase mass transfer

* Corresponding author. Tel.: +35928703273; fax: +35928707523
E-mail address: mixreac@bas.bg

applications. The modifications were aimed at increasing streamlining and providing openings and slots for pressure recovery. The first group is represented by cases CB and SCB and the second group is represented by PFB, SFB and SCB. An excerpt of the set of designs considered is shown schematically in Fig. 1. The abbreviations mean: conventional flat blade (**FB**), semi-circular (Smith) blade (**CB**), slotted flat blade (**SFB**), perforated flat blade (**PFB**), and slotted semi-circular blade (**SCB**). Designs FB, CB and PFB met prototypes in papers by Rushton, Warmoeskerken and Smith,[15] and Roman *et al.*[16] The concave version of CB was examined.

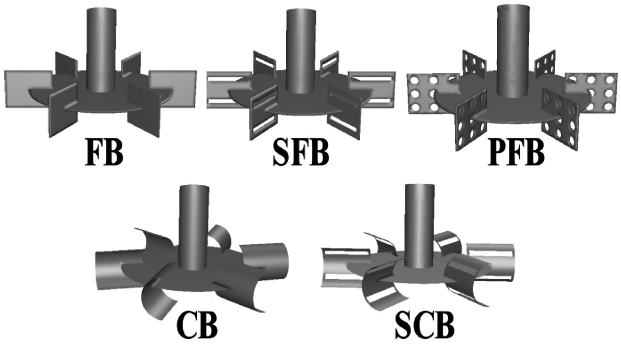

Fig. 1 – *Schematics of blade designs*

The physical model setup included a stirred vessel with diameter T = 0.4 m with a single impeller sized $D = T/3$ and located centrally. All blades were standard in size. Liquid height was $H = T$. All designs were tested at $Re > 10^4$ in water at $n_s = 600$ min^{-1}.

Numerical simulation

The impeller performance in the turbulent regime was examined. In order to include the fluctuations u' of mean velocity U in the Navier-Stokes equations, time-averaging of the momentum conservation equations was used that yielded new variables, namely, the Reynolds stresses $\overline{u_i' u_j'}$, and set of the Reynolds-averaged Navier-Stokes equations (RANS). To close the solution, the semi-empirical two-equation "k-ε" turbulence model balancing the turbulence kinetic energy k and rate of energy dissipation ε, was used. The model equations are well established and for a detailed review one could follow reported summaries. In this study, the commercial code FLUENT 6.1.22[17] was used.

The computational models contained 3D-grids with a total of up to 800 000 mixed hexahedral, quadrilateral and triangular cells. The meshes of the different design cases were structured identically by using a commercial code (GAMBIT version 2.1.6, Fluent Inc.). Grid refinement around the impeller walls was applied, as illustrated in Fig. 2.

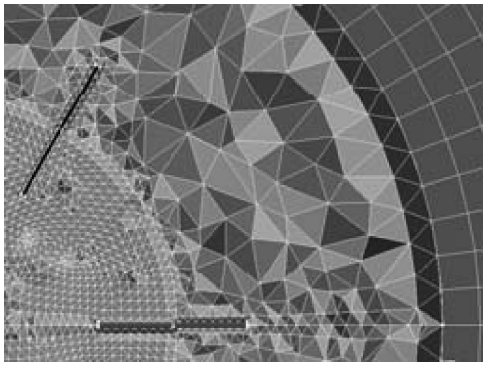

Fig. 2 – *Grid refinement near the impeller*

In view of impeller rotation, the flow in a stirred tank is solved separately within an inner rotating region and an outer stationary region.[18] A small inner volume was defined with a boundary interface over which the two solutions communicated. First, the flow characteristics of the inner region were solved using a rotating framework. These results were used as boundary conditions for the outer (stationary) framework. Iteratively, the solution of the outer frame region referred to the solution of the inner frame region and vice versa until converged solution was reached (within the set of "reference frames" i.e. the multiple reference frame (MRF) model. Following a second order upwind differencing scheme of discretization, the number of iterations reached ca. 3 000.

Convergence criterion of 10^{-4} was assumed. The iterations were started by substitution of zero velocity and turbulence kinetic energy and dissipation rate equal to 0.001. The under-relaxation factor was set to 0.5 for pressure and 0.2 for momentum.

The power number, Po, was determined based on the torque M imposed by the impeller to the fluid: $Po = 2\pi n_s M / (\rho\, n_s^3 D^5)$. The momentum centre coincided with the intersection of the shaft (z-axis) and the horizontal impeller plane. The flow number ($Fl = Q_l / n_s D^3$) was determined by integrating the radial impeller outflow, $Q_l = \int \pi \mathrm{d} h v_r$ over a cylindrical surface.[19] Velocity v_r and turbulent intensity Tu were angle-resolved over the various planes crossing the z-axis.

Physical experiments

In particular, to examine mixing effectiveness, the power and the gas-liquid mass transfer coefficient for oxygen transfer were measured. The power numbers were determined following experimental measurement of power. A measurement system comprising a sensor for torque and telemetric control (Electroinvent®) was employed. The sys-

tem was tested by comparing its output with other reference sets reported in.[20]

The gas-liquid mass transfer was evaluated by the dynamic measurement technique. Single dissolved oxygen probe has been involved, as reported previously.[21] The dynamic response of the liquid phase was evaluated by the MM model,[22] assuming complete mixing regimes (M) for both the gas and the liquid, as appropriate for intensive vessels:

$$D_R = (R_t\text{-}R_0)/(R_s\text{-}R_0)$$

Where, R is the probe response at saturation (R_s), at $t = 0$ (R_0) and at time t (R_t). The k_La –value was determined as the slope of a linear function ln ($1\text{-}\ D_R$) versus t. The probe (Ingold) dynamic response and constants have been considered.[23] The relative mean deviation of k_La, as measured by this technique was 8.5 %.

Validation examples

Validation of the RANS "k-ε" model solutions has been carried out by various authors; the model has been evaluated positively for design purposes.[9,10,24] Consequently, the validation in this study was focused on the specific grids and Gambit models of the impeller geometries employed. Experimental and reference data including power number *Po*, external flow deformation rate ω and flow number *Fl* were compared. For example, the value *Po* = 5.67 obtained by CF simulation for FB mixing in water and *Po* = 3.16 for CB in water compared well with the reference values of 5.5 ± 0.5 for Rushton[19,25] and 3 ± 0.3 for Smith.[25] Similarly, the model-obtained *Fl* = 0.86 for case FB compared well with the reference value *Fl* = 0.75 ± 0.15 reported for Rushton turbine[25] and the model-obtained CFD *Fl* = 0.77 of case CB compared well with the reference value *Fl* = 0.76.[19] The value for the FB deformation rate (6600 s^{-1}) obtained by CFD compared well with the value 7000 s^{-1} measured on flat blades by Wichterle and coworkers.[26]

Results and discussion

Table 1 presents a summary of the mixing macro-parameters, i.e. the impeller power and flow numbers. It is noteworthy that, in so far as it is based on comprehensive torque computation, *Po* obtained by CF simulation is an accurate parameter in contrast to experimental *Po* values that may show considerable scatter. Thus, the model-obtained *Po* value was considered, as highly informative with respect to the drag-velocity relationship of the relevant design modification.

Table 1 – *Power numbers and flow numbers*

Impeller	FB	CB	SFB	PFB	SCB
Po	5.67	3.16	3.51	3.54	2.64
Po (exp)	5.5 ± 0.5[18]	3 ± 0.3[15]			
Fl	0.86	0.77	0.71	0.74	0.70
Fl (exp)	0.75 ± 0.15[18]	0.76[15]			
Po/Fl	5.48	3.4	4.11	3.97	3.12

Table 1 shows *Po* variability in the range 2.6–5.67, the minimum power number corresponding to the slotted half-pipe impeller (SCB) and the maximum one – to the conventional flat blade turbine (FB). The perforated blades (PFB) and the slotted blades (SFB and SCB) exhibited lower power requirements than the compact designs FB and CB. With the ratio *Po/Fl* > 2.5, all impellers belonged to the shear type.[27]

In order to check if the pumping capacity was maintained, *Po* was confronted with *Fl* in the Table. Practically equal circulation rate in all cases was registered. Thus, the decrease of the power number was not a matter of a decreased effective pressure drag, but rather a matter of decreased pressure losses.

Pressure recovery has been sought by simulation post-processing over the blades' shadow. The pressure at the blades' rear was examined. The pressure difference with respect to the zero pressure at the blades was represented by pressure coefficients $C_p = \dfrac{2\Delta p}{\rho v_t^2}$, as illustrated in Fig. 3.

As expected, the conventional flat blades showed wide low-pressure zones indicating adverse

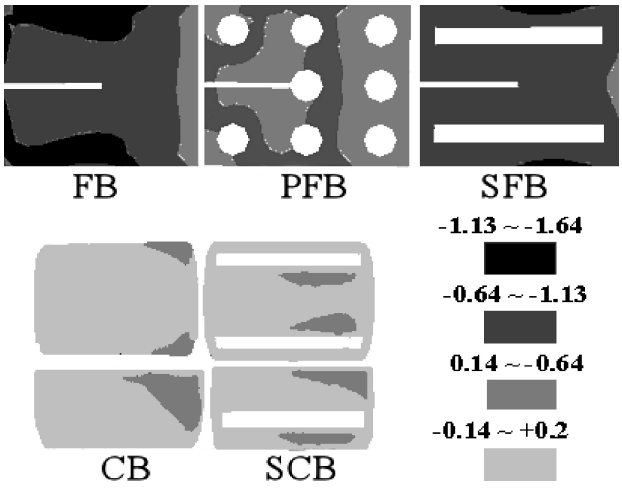

Fig. 3 – *Pressure distribution at the blades' rear*

pressure gradients amenable to flow separation and kinetic energy loss. Accordingly, an increased power requirement is known to be specific for this impeller.

The pressure distribution corresponding to the modified blades showed improvement of this parameter, especially in so far as the perforated designs were concerned. The pressure recovery at the blades' rear is indicated by the shrinking or disappearance of the low pressure (black) zones. The slot effect was probably due to flow acceleration and kinetic energy gain in the openings hindering separation and rotational (vertical) flow.[12] The effects were better pronounced for blades with curved 'streamlined' boundaries, e.g. CB and SCB; these showed even positive pressure coefficients' zones, something that explained their low power number.

Further, the specific deformation rates were studied. Area-weighed average strains over planes crossing the z-axis are shown in Fig. 4. Table 2 contains the mean strain rates ω_b and ω_i, obtained as volume-weighted average values over the bulk and the impeller zones, respectively. (The impeller zone was a cylinder inscribed over 10 % of the overall liquid volume centered at the impeller zero level).

The strain rate differences were significant in the impeller zone (ω_i) and varied within 25 % in the bulk area of the stirred vessel (ω_b). Because dispersion capacity is related to deformation, high dispersion capacity could be assigned to the cases of high impeller strain, e.g. in case PFB according to the data. The parameter is important also in cases of shear-sensitive biomass. Unexpectedly, FB showed high only in the bulk fluid.

Table 2 – *Impeller-induced strain rate and power effectiveness*

Impeller	e_V [W dm^{-3}]	ω_i [s^{-1}]	ω_i/e_V [J^{-1} dm^3]	ω_b [s^{-1}]	ω_b/e_V [J^{-1} dm^3]
FB	4.71	368	78.1	21	4.45
CB	2.62	213	81.3	18	6.87
SFB	2.92	453	155	18	6.16
PFB	2.94	389	122	19	6.46
SCB	2.19	266	121	17	7.76

Referring to dispersion in multiphase flow, also turbulent intensity is important. Fig. 5 presents the *Tu* profiles corresponding to the different designs. In these studies, turbulence intensity was determined as $Tu = \left(\sqrt{\frac{2}{3}k}\right)/v_t$ where k is turbulence kinetic energy and v_t is the reference (tip) velocity, $v_t = 4.18$ m s^{-1}.

Unidirectional with FB, again SFB and PFB cases were sound. However, as discussed earlier[24] the RANS models address a time-averaged state of the fluid such that all turbulent fluctuations are represented by averaged values. Thus, they are not enough accurate to capture small scale turbulent eddies' fluctuations. Consequently, we have refrained from detailed interpretation. The mass transfer coefficients have been compared, instead. Physical experimental results on oxygen transfer using FB, SFB and PFB are compared in Fig. 6. While k_La deviation is within 15 % that is comparable with the

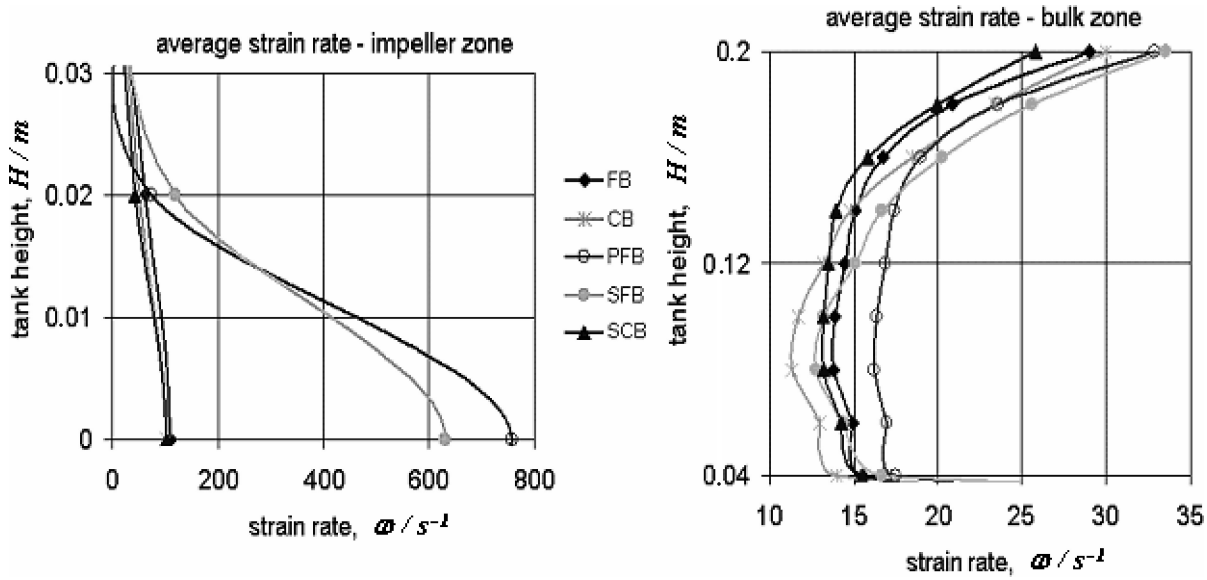

Fig. 4 – *Strain rate distribution corresponding to the blade designs*

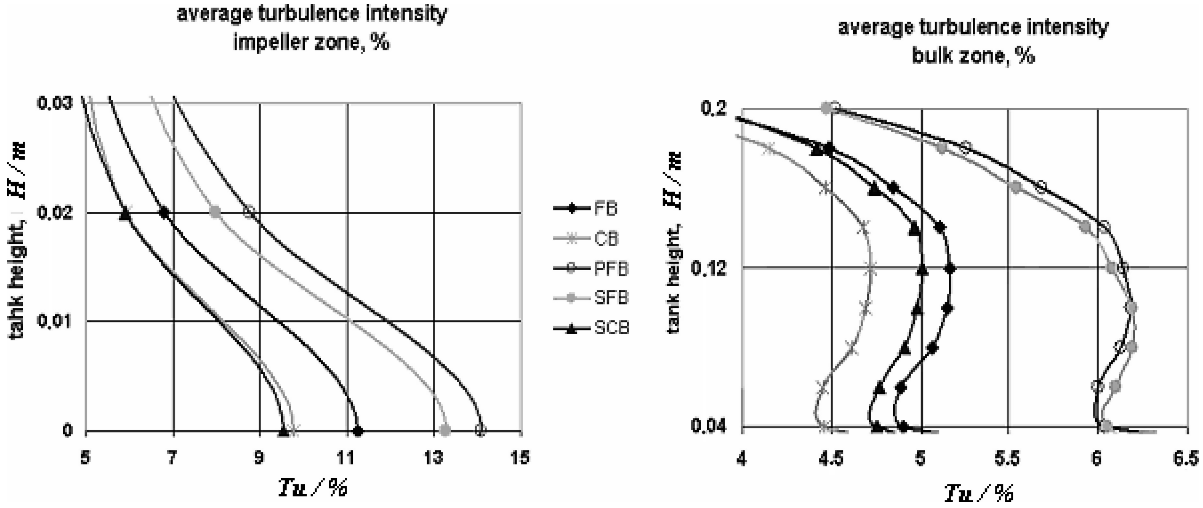

F i g . 5 – *Distribution of average turbulence intensity corresponding to the blade designs*

measurements' relative error, a trend towards mass transfer enhancement in the slotted case is seen clearly to conform to the lower power requirement at preserved mixing efficiency for these specific cases. For a similar case of perforated flat blades in a slightly different fashion, i.e. two rows of openings instead of three at D_i = 5 mm, Van't Riet and Smith[11] reported unidirectional results of a 30 % increase of the gassed power ratio compared to the non-modified version.

Finally, the power effectiveness estimated as strain rate per unit input power was examined. Table 2 contains the results. Practically in all cases, the data shows close values of bulk strain rates ω_b. The trend stands different for the impeller zone, i.e. for ω_i. On the other hand, the perforations and the slots count for a 2-fold increase of the near-impeller deformation effectiveness (compare ω_i/e_v in cases FB and SFB, PFB, respectively) and of up to a 50 % increase in bulk effectiveness (compare ω_b/e_v in cases FB and PFB, as well as CB and SCB). In view of the different power requirement, also the specific mixing effectiveness is different; it is higher in cases PFB, CB and extremely high in case SCB. By comparing the data obtained for curved and flat shapes, one may infer that designing perforations and slots on the blades is no less important than improving streamlining, e.g. relevant in the case of Smith blade (CB).

Reaction evidence conforming to this observation has been presented by Roman and coworkers (1996).[16] These authors have shown more than 30 % increase of relative antibiotic production in fermentations of *Strepromyces aureofaciens*, *Streptomyces rimosus* and *Penicillium chrysogenum* producing tetracycline, oxytetracycline and penicillin antibiotics in bioreactors equipped with impellers similar to the PFB version studied.

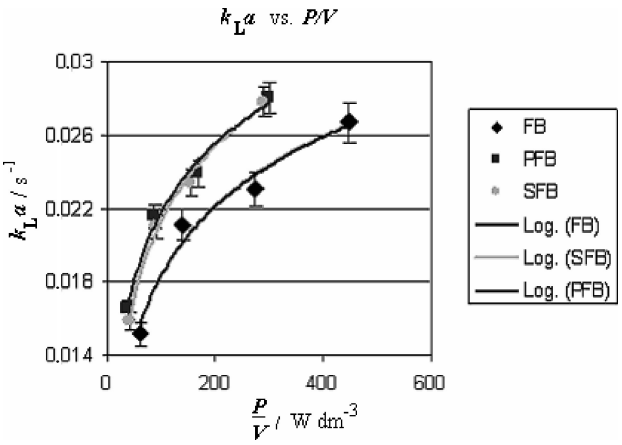

F i g . 6 – *k_La vs. P/V for the flat blade designs*

Conclusion

The flow field differences imposed by perforation and slotting of the impeller flat blade design have been revealed. The power requirements, pumping capacity, deformation rate and turbulence intensity of the modified impellers were identified and compared. The slotted and perforated blades are found to decrease relevant power requirements and increase deformation impacts. While preserving the pumping capacity, the slotted blades show up to 40 % lower power requirement and up to 20 % higher deformation rates than conventional compact blades. Gas-liquid mass transfer rate of slotted flat blade has been measured and shown to preserve and even improve conventional flat blade characteristic. The higher performance of the slotted design is found to correlate with pressure recovery evidenced on the blade shadow. The study points at using the studied designs further as options for increased energy-saving in mixing operations by retrofitting impeller units in industrial-scale reactors.

Symbols

C_p – pressure coefficient
D – impeller diameter, m
e_v – volumetric input power, W dm^{-3}
Fl – flow number, $Q_l / n_s D^3$
H – liquid height, m
k – turbulence kinetic energy, m^2 s^{-2}
M – torque, N m
n_s – impeller speed, min^{-1}
Po – power number, $P / n_s^3 D^5 \rho$
Q_l – liquid pumping flow rate, m^3 s^{-1}
Re – impeller Reynolds number, $\rho n_s D^2 \mu^{-1}$
ω – strain rate, s^{-1}
T – tank diameter, m
Tu – turbulence intensity, %
v – velocity, m s^{-1}
μ – dynamic viscosity, Pa s
ρ – density, kg m^{-3}

Indices

b – bulk
i – impeller
r – radial
t – tangential tip

Abbreviations

RANS – Reynolds-averaged Navier-Stokes (equations)
MM model – assuming complete mixing of both phases (model)
MRF approach – assuming solution iterations intra two or more frameworks of grids, e.g. two grids – a rotating one and a stationary one

References

1. Shell Report 2004. Royal Dutch Shell Group Co., www.shell.com.
2. *Fort, I., Medek, J., Ambros, F.*, Chem. Biochem. Eng. Q. **13** (1999) 127.
3. *Orvalho, S. C. P., Vasconcelos, J. M. T., Alves, S. S.*, Proc. 10th Eur. Conf. on Mixing (Delft), Elsevier, Amsterdam, 2000, pp 461- 468.
4. *Pinho, F. T., Piqueiro, F. M., Proenca, M. F., Santos, A. M.,* Chem. Eng. Sci. **55** (2000) 3287.
5. *Vlaev, S. D., Mavros, P., Seichter, P., Mann, R.,* Can. J. Chem. Eng. **80** (2002) 653.
6. *Khopkar, A. R., Ranade, V. V.,* Proc. 11th Eur. Conf. on Mixing (Bamberg), VDI-GVC, Dusseldorf, 2003, pp 487–493.
7. *Pinelli, D., Bakker, A., Meyers, K. J., Reeder, M. F., Fasano, J., Magelli, F.,* Trans. IChemE **81** (A) (2003) 448.
8. *Szalai, E. S., Arratia, P., Johnson, K., Muzzio, F. J.,* Chem. Eng. Sci. **59** (2004) 3793
9. *Kumaresan, T., Joshi, J. B.,* Chem. Eng. J. **115** (2006) 173.
10. *Joshi, J. B., Ranade, V. V.*, Ind. Eng. Chem. Res. **42** (2003) 1115.
11. *Van't Riet, K., Smith, J. M.*, Dechema Monographien **74** (1974) 93.
12. *Smith, J. M.,* In Ulbrecht, J. J., Patterson, G. K. (Ed.), Mixing of Liquids by Mechanical Agitation, Gordon and Breach, New York, 1985, pp 139–201.
13. *Georgiev, D., Vlaev, S. D.*, Flow field variation by minor modification of impeller blades, in Magelli, F., Baldi, G., Brucato, A. (Ed.), Proc. 12th Eur. Conf. on Mixing (Bologna), AIDIC, Milano, 2006, pp 41- 48.
14. *Shames, I.*, Mechanics of Fluids, 3d Ed., McGraw-Hill Publ., New York, 1992.
15. *Warmoeskerken, M. M. C. G., Smith, J. M.*, Chem. Eng. Res. Des. **67** (1989) 193.
16. *Roman, R. V., Tudose, Z. R., Gavrilescu, M., Cojocaru, M., Luca, S.*, Acta Biotechnol. **16** (1996) 43.
17. Fluent Inc., Fluent 6.1 Documentation. CD, New Hampshire, 2003.
18. *Brucato, A., Ciofalo, M., Grisafi, F., Micale, G.*, Chem. Eng. Sci. **53** (1998) 3653.
19. *Paul, E., Atiemo-Obeng, V., Kresta, S.,* (Eds.), Handbook of Industrial Mixing-Science and Practice, Wiley, New Jersey, 2004.
20. *Mezaki, R., Mochizuki, M., Ogawa, K.,* Engineering Data on Mixing, Elsevier Science, Amsterdam, 2000.
21. *Martinov, M., Vlaev, S. D.*, Chem. Biochem. Eng. Q. **16** (2002) 1.
22. *Nocentini, M.,* Trans. Inst. Chem. Eng. **68A** (1990) 287.
23. *Vlaev, S. D., Valeva, M.*, J. Biotechnol. **11** (1989) 83.
24. *Hartmann, H., Derksen, J. J., Montavon, C., Pearson, J., Hamill, I. S., Van den Akker, H. E. A.,* Chem. Eng. Sci. **59** (2004) 2419.
25. *Tatterson, G. B.,* Fluid Mixing and Gas Dispersion in Agitated Tanks, McGraw-Hill, New York, 1991.
26. *Wichterle, K., Kadlec, M., Zak, L., Mitschka, P.,* Chem. Eng. Commun. **26** (1984) 25.
27. *Nagata, S.*, Mixing: Principles and Applications, Wiley, New York, 1975.